

31 INTRODUCTION

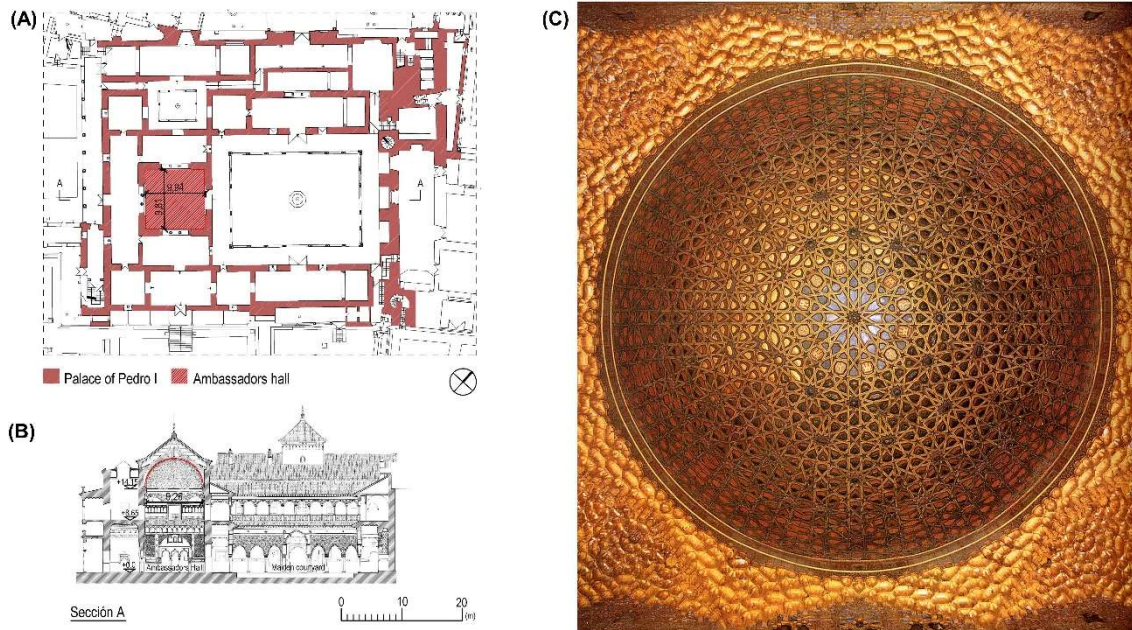
32 **Subject and Purpose of the Research**

33 The object of this study involves the wooden dome in the Hall of Ambassadors of the Real Alcázar
34 of Seville (Spain) built in 1427 AC. Three objectives can be indicated in this research: first, the
35 completion of an in-depth description of the geometry of the dome and its constructive configuration,
36 thereby complementing the current descriptions that adhere to its merely formal and stylistic aspects;
37 second, the establishment of a hypothesis of the procedure carried out for the construction and assembly
38 of the dome; and third, an analysis of its structural behaviour, for which a three-dimensional model is
39 developed. Before tackling these objectives, an overview of the historical construction of wooden domes
40 is presented and, specifically, a description is given of the cultural and knowledge context in which the
41 construction of this dome is situated.

42 **Preliminary Description, Situation, and Historical Context**

43 The Real Alcázar of Seville comprises a walled enclosure within which buildings constructed
44 mainly between the 9th and 15th centuries are preserved, although they do have Roman antecedents and
45 underwent extensions and reforms up to the 19th century. The main building is known as the *Palacio de*
46 *Don Pedro* wherein the Hall of Ambassadors is located, whose dome is the object of this research (Figure
47 1 A and B). Since 1987, the complex has been inscribed onto the UNESCO World Heritage List. This
48 palace was built between the years 1364 and 1369 CE. Later, during the reign of Juan II (1405-1454), the
49 construction of emblematic pieces, such as the Hall of Ambassadors and its dome, was carried out.
50 According to an inscription found on the dome itself, its author was the Master craftsman of King Diego
51 Ruiz in 1427 (González de León, 1844).

52 This is a dome built entirely with wooden elements that includes a complex interlacing pattern,
53 based on the geometry of 10-point stars, that runs along the entire surface of the dome (Figure 1C). Its
54 design and construction form part of the long-standing traditional Spanish structural carpentry.
55 Stylistically, it can be ascribed to the so-called “Mudejar” style, whose meaning alludes to the
56 identification of a specific artistic style, and not as a term ascribable to a specific ethnic or social
57 authorship.



58

59 *Figure 1: (A) Ground floor of the Real Alcazar of Seville with the Palace of Pedro I and Ambassadors*
 60 *Hall highlighted. (B) Section A: Palace of Pedro I through the Ambassadors Hall and the Maiden*
 61 *courtyard. (C) Wooden dome over the Ambassadors Hall. Overhead view.*

62 The dome is located on a space of approximately square proportions, 9.25 m on each side. The
 63 walls of this space, built with solid brick, have an average thickness of 0.90 m. The spring line of the
 64 dome is produced at an elevation of +14.15 m above the ground. For the transition between the square
 65 ground plan of the wall structure and the circular ground plan of the dome, wooden squinches are created
 66 in the corners decorated with clusters of muqarnas.

67 The structure of the dome is protected from the elements by a covering, probably not original,
 68 comprised of a wooden octagonal roof framing covered with ceramic tiles.

69 **WOODEN DOMES: BACKGROUND AND REFERENCE STUDIES**

70 **References and Studies on Wooden Domes**

71 Since ancient times, the construction of domes has utilised discrete elements, brick or stone, with
 72 numerous references available in the scientific literature regarding their configuration and structural
 73 behaviour. However, knowledge regarding timber as a structural element in domes remains scarce, owing
 74 to its limited usage therein. This low level of utilisation may have been due to the constructive complexity
 75 of the processes involved (bending of the wood, assembly, difficulty of geometric control) or to the lack

76 of forested land, and hence the lack of any constructive tradition in carpentry in certain geographical areas
77 (Almagro, 2001).

78 An indication of the existence of domes and vaults built with timber which have since disappeared
79 can be found in classical Greece. Misztal (2018, p. 7) refers to the Aeschylus Temple in Epidaurus (370
80 BCE) and indicates that *“the slight thickness of masonry, stone walls allows to presume that light,
81 wooden roofs were resting on them. The spacing of walls and pillars shows that it could not be simple
82 beam roofs”*.

83 A large group of disappeared domes built in wood deserve mention, which are precisely the
84 temporary frameworks destined to become an auxiliary means for the construction of stone or brick
85 domes. The few articles that refer to old domes featuring timber classify them primarily according to their
86 number of layers (simple or multi-shell domes) (Misztal, 2018; Ashkan and Ahmad, 2010). From the
87 point of view of its structural functioning, in domes built with timber, differentiation should be made
88 between membrane-type domes and truss-type domes; and intermediate states (hybrid double domes) can
89 be considered where wood, despite being a secondary element, plays a major role (Tavakoli et al., 2019).

90 Perhaps the oldest wooden dome for which there are specific references is the Qubbet al-Sakhrah
91 (The Dome of the Rock) in Jerusalem, built circa 687-692 CE. Few references to the constructive
92 composition of its dome are in existence; most references reproduce the magnificent drawing by De
93 Vogue (1864), which represents the existence of two layers of wooden elements that remain joined at the
94 dome crown. This, however, could not be its initial configuration. Indeed, Necipoğlu (2008, pp.31) states
95 that *“the collapsed cupola was rebuilt in 1022-23”*, and, more recently, al-Ratrouf (2017) has provided
96 further data. Along these lines, the dome over the al-Aqsa mosque (Jerusalem, Israel, 715 CE), also
97 rebuilt circa 1035 CE, deserves mention. The structure of its outer layer stands out with a simple and
98 effective system of ribs arranged according to the meridians of the sphere, which are strengthened with
99 cross bracing elements arranged according to the diagonals of the panels. As in the Dome of the Rock
100 Mosque, the interior structure hangs from the upper structure through a connection in its crown.

101 To the best of our knowledge, there are no other examples of complete wooden domes in the Islamic
102 world. In Iran, where there is a long tradition of building domes, wood can be found as a secondary
103 element in double-layer domes for the purpose of stiffening or connecting the interior and exterior layers
104 built with brick (Ashkan and Ahmad, 2010). One exception could be the dome of the Esfahan Shah

105 Mosque (Iran). In Miształ (2018), this dome appears as a large wooden load-bearing structure that
106 supports layers of the interior and exterior fabric. However, a more recent and detailed analysis (Tavakoli
107 et al., 2019) defines it as a hybrid double dome, where the timber, despite being indispensable, appears
108 only as a connecting element.

109 In the West, the five domes of the Basilica of San Marco in Venice, built in the mid-13th century,
110 could constitute the oldest references, despite having been at least partially rebuilt after the fire of 1419.
111 In the work of Fregonese et al. (2009), the structure of the Pentecost dome is clearly shown. This involves
112 a framework of wood in which three levels of horizontal rings are of note, attached to a central king post
113 and large inclined straight beams that span from the key structural compression ring to the base. On the
114 set of rings, thin ribs form the domed outer surface.

115 Subsequent to this antecedent, no dome construction took place the mid-15th century when several
116 domes were built in Veneto with wooden structures. Piana (2009) provides an interesting account of these
117 constructions: most continue with systems similar to the domes of San Marco, such as that of San Giovanni
118 e Paolo (1430) and Santa Maria dei Miracoli (c. 1485). An exceptional case is that of the dome of the
119 Church of San Pietro in Castello (mid-16th century), with its single-layer membrane formed by thin
120 wooden meridian ribs very close to each other connected transversely by numerous noggings that follow
121 the parallels of the dome. This structure is the only construction that is found to be similar in any way to
122 our dome in the Hall of Ambassadors. Later, Palladio, with greater efficiency, recovers the initial system
123 of San Marco, with double-layered domes with two parallel chords joined together by perpendicular
124 counterbraces in San Giorgio Maggiore (1576) and with a hinted triangulation in the Church of the
125 Santissimo Redentore (1592).

126 Along these lines, close in time, but with very different constructive approaches, Philibert de
127 L'Orme's "Nouvelles inventions" appeared in 1561, wherein, although in the context of vaults, the
128 possibility of their execution with a membrane behaviour is initiated. The double-layer parallel system is
129 later rarely used and gives way to the appearance of systems characterised by the location of trusses in the
130 meridians, where the timber chords located in the upper and lower layers together with cross bracing
131 between them form a stable and efficient structure. Examples of this are given by the domes of Santa
132 Maria della Salute in Venice (1687), the dome in the Church of the Invalides (Paris, France, 1693–1706),
133 the new dome of St. Paul's Cathedral (London, England, 1710), or the Schönborn Chapel (Würzburg,

134 Germany, 1722). Antecedents of these systems are collected in various treatises, such as those by Jousse
135 (1627) and Le Muet (1681).

136 In Spain, evidence shows that, from the 17th century, the constructive configuration of domes has
137 followed the same trends as in the rest of Europe, highlighted by the texts of García Berruguilla (1747)
138 and Bails (1796), in which vaults built with truss systems are drawn. However, another system had been
139 developed in Spain in the Middle Ages and at the beginning of the Renaissance, with no historical
140 reference to another era or region: domes featuring interlacing patterns. These are single-layer domes
141 made up of wooden elements that follow a precise geometry governed by an interlacing design based on
142 regular stars. Their structure and ornamentation are inextricably fused with great precision to form the
143 supporting structure, a unique and distinctive feature of the Hispanic carpentry tradition and characteristic
144 of Mudejar art. Only four domes of this type exist in the whole world, of which the largest and oldest is
145 discussed in this article. The other three domes are the dome of the Duques de Maqueda Palace in
146 Torrijos, Toledo, built at the end of the 15th century and currently housed at the National Archaeological
147 Museum of Madrid (Nuere Matauco, Candelas-Gutierrez, and De Mingo García, 2020), the dome over
148 the main staircase of the “Casa de Pilatos” in Sevilla (1538), and the dome built in the convent of San
149 Francisco de Lima (Peru). In the latter case, the original was destroyed in the Trujillo earthquake of 1725.
150 Later rebuilt, due to its poor state of conservation, it collapsed again in the 1940 Lima earthquake. The
151 current dome is from the late 20th century, built by the Peruvian architect Alberto Barreto Arce.

152 **Cultural Context and Previous Constructive Knowledge**

153 Knowing how to build a wooden dome was the highest degree to which a member of the powerful
154 medieval guild of traditional Spanish structural carpenters could aspire. Whoever reached such a level
155 could hold the rank of *Iumetrico*. This is stated in the ordinances of the guild that were later included in
156 the city ordinance of Sevilla in 1527 (Varela de Salamanca, 1527). The knowledge utilised by medieval
157 carpenters in Spain, transmitted orally, came to light in later texts by López de Arenas (1619 and 1633),
158 in a manuscript by Fray Andrés de San Miguel (early 17th century), and in the manuscript by Rodrigo
159 Alvarez (1699). Diego López de Arenas, in his text of 1633, and Fray Andrés de San Miguel (c. 1640),
160 both in the final part of their writings, address the construction of these domes.

161 The text by López de Arenas contains the procedures with which the carpenters were able to build
162 resistant frameworks based on the rafter and collar-beam system, into which widely different interlacing

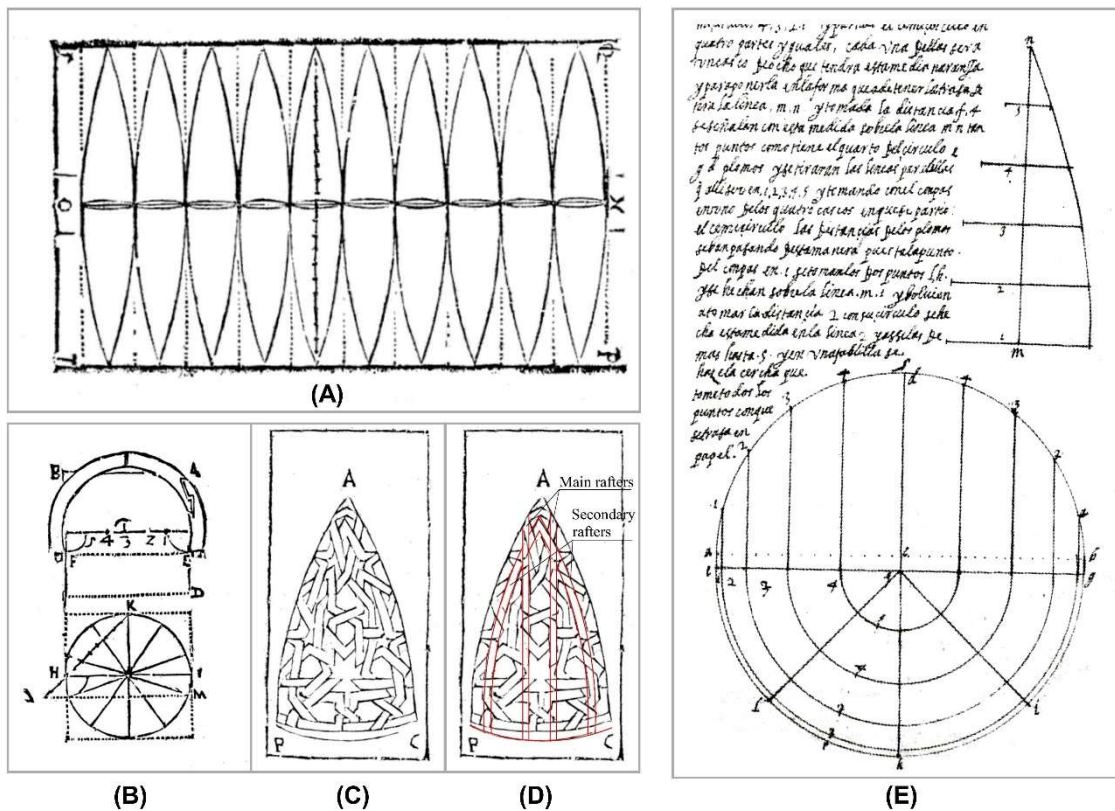
163 configurations could be incorporated as an integral element of the structure. All this provides an
164 extremely interesting contribution: the possibility of prefabricating large areas of the structure in order, on
165 the one hand, to facilitate the complex insertion of interlacing patterns into the framework, and, on the
166 other hand, to be able to carry out an efficient assembly in situ. This was achieved on roofs with three or
167 more planes by duplicating the hip rafter, so that each sector had a precise physical limit and sufficient
168 stiffness and stability prior to lifting and mounting.

169 The case of these wooden domes is in fact a particular case of the evolution of the rafter system, in
170 which a few main curved rafters serve as a fundamental continuous element. A series of secondary curved
171 rafters are placed in the strict position required by the interlacing geometry that is being incorporated into
172 the structure, all joined with a mesh of noggings that, following the interlacing pattern, join the main and
173 secondary rafters, thereby forming a membrane with a highly effective structural behaviour.

174 The text by López de Arenas (1633) includes several geometric descriptions for the execution of
175 what he calls a “half orange” that is, a hemispherical dome with an expansion somewhat greater than the
176 semicircle. Its cross-section resembles a horseshoe arch and gives the name “bolsor” to the sector of the
177 sphere that exceeds the line of the equator.

178 For its construction, López de Arenas proposes the division of the dome into sectors, and
179 exemplifies the process with a sphere divided into ten spherical triangles, and includes the following
180 drawing (Figure 2A), in which, with rudimentary knowledge, he strives to transfer spherical geometry
181 into plane geometry. This author also contributes another interesting drawing in which a section of the
182 dome is represented (Figure 2B). The drawing presents two definitions: on the one hand the length of the
183 “bolsor” and, on the other hand, an attempt to describe the length of the main rafters. He defines the
184 “bolsor” with a cant length equal to $1/6$ of the diameter. To obtain the length of the main rafters, he
185 indicates in the text that he is going to apply “*proposition 32 of the first book of Archimedes*” while
186 utilising the relation $22/7$ as an approximation to the number Pi. The figure incorporates other important
187 details. On the one hand, the tenon that appears in the lower part of the beam that joins the curved rafter
188 with the wall plate can clearly be seen. On the other hand, there are two joints: an abutting joint at the
189 upper purling structural ring, and a stop-splayed scarf joint at an intermediate point of the arc. In another
190 drawing of the same text (Figure 2C), López de Arenas represents a sector of the sphere with the
191 introduction of interlacing patterns. In Figure 2D, based on this drawing, the location of the underlying
192 structural elements has been represented, in which the duplication of the secondary rafter is utilised, each

193 sector thereby providing a solid outline that would allow its on-site assembly and its subsequent lifting
 194 into its final position.



195 (B) (C) (D) (E)
 196 Figure 2: (A, B, C, D) Drawings from the 1633 text of Lopez de Arenas. (E) Drawings from the
 197 manuscript of Fray Andres de San Miguel.

198 Fray Andrés de San Miguel dedicates the last pages of the part of the manuscript on carpentry to the
 199 vaulted forms. That manuscript was fully studied in Nuere Matauco (1990). The approach by Fray Andrés
 200 is more focused on the geometric description of these domes than on their constructive materialisation,
 201 although in this regard, data of interest is also included. The objective pursued by Fray Andrés in the
 202 spherical vault involves obtaining a flat surface upon which to develop the interlacing pattern. In the same
 203 way as by López de Arenas, this approximation to a flat shape is carried out by displaying a sector of the
 204 sphere between meridians. To this end, Fray Andrés uses a division of the sphere into 8 sections, instead
 205 of the 10 utilised by López de Arenas. His proposal is very simple, since it is based on obtaining the
 206 longitude of a meridian, dividing it into n parts, and transferring to these divisions the length of the arcs
 207 corresponding to the height of each division.

208 The geometric description of the process described by Fray Andrés is much more exact than the
209 incomplete proposal by López de Arenas. However, Fray Andrés fails to include the drawing of any
210 sample of the interlacing pattern in his assertions, nor does he introduce any description of the
211 materialisation of a framework constructed in this way. In fact, the drawing provided (Figure 2E) remains
212 totally detached from any reference to construction elements.

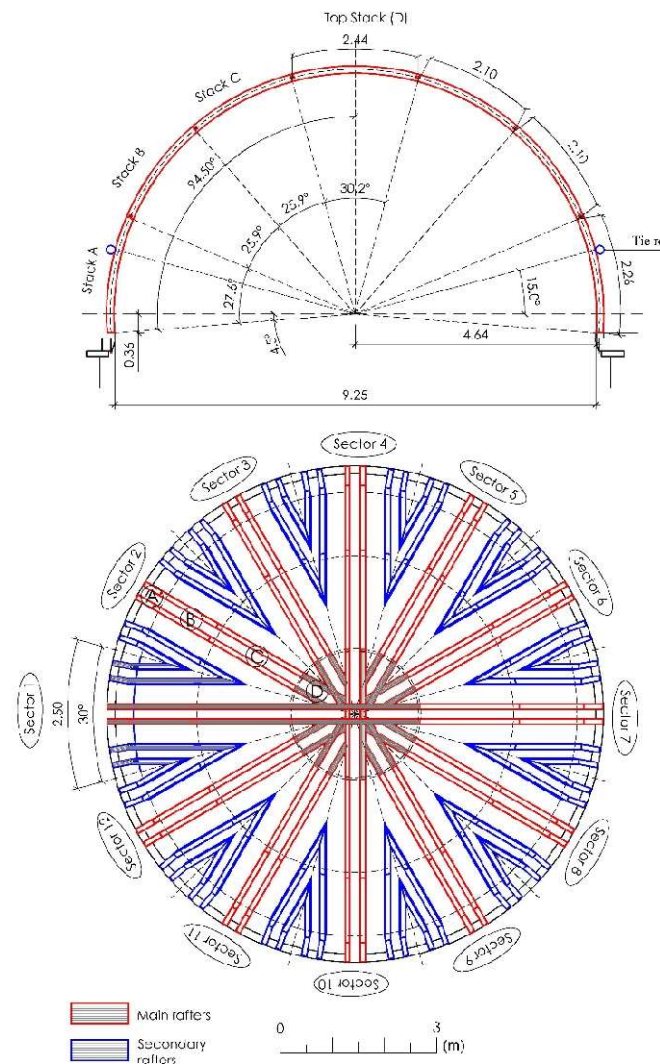
213 **DESCRIPTION OF THE DOME OF THE HALL OF AMBASSADORS**

214 **Geometry and Constructive Configuration**

215 The section of the dome is ultrasemicircular; its profile extends 4.5° from the equator, and hence its
216 cross-section is, in fact, a horseshoe arch. In this way, the inside diameter of the 9.28 m sphere is slightly
217 reduced at the springline to 9.25 m. The length of the “bolsor” (basilar superelevation) is 0.36 m.

218 Its configuration can be understood as the repetition of 12 spherical triangles (sectors) around the
219 zenith of the sphere. Each of these spherical triangles is made up of 3 spherical trapezium-shaped zones
220 that are joined together (stacks A, B, and C in Figure 3). These sectors do not converge at the crown of
221 the dome but end at a distance of 1.22 m from the pole of the theoretical sphere. For this reason, for the
222 closure of the spherical surface in its upper part, a last sector is utilised in the shape of a spherical cap
223 (stack D in Figure 3), which, in the form of a keystone, completes the dome. Each sector is made up of 2
224 main rafters of geometric continuity, although not physically present all the way up to the upper stack. In
225 this way, only 12 rafters start from the wall plate and reach the upper stack, while another 60 secondary
226 rafters start from the base but end up converging with each other.

227 The arrangement of the rafters is closely related to the interlacing pattern tracing that runs across the
228 entire surface of the sphere. It is a design based on the concatenation of 10-point stars with their
229 corresponding wheels that converge in the upper spherical cap, thereby generating a large central 12-point
230 star.



231

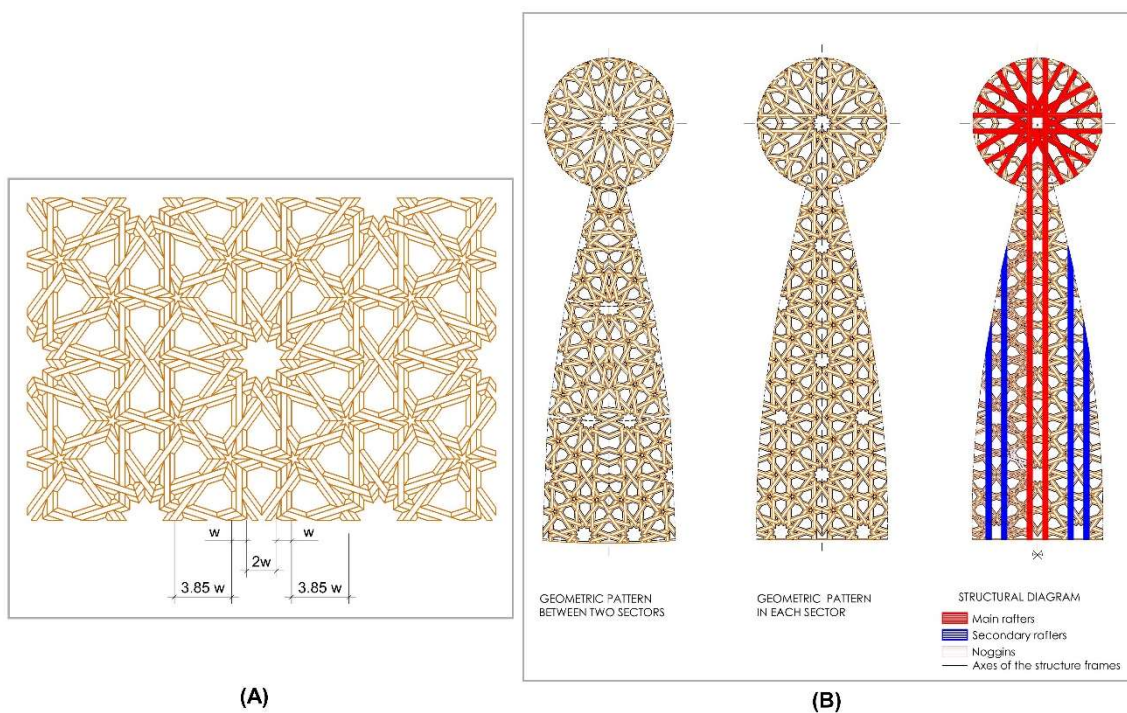
232 *Figure 3: Geometrical diagram of the wooden structure of the dome. Middle section and plan. The main*
 233 *and secondary rafters are indicated.*

234 The carpenter who built this work faced three major difficulties: first, the handling of spherical
 235 geometry; second, the introduction therein of the rigid geometry of the interlacing pattern; and third, the
 236 need for structural capacity. The interlacing pattern of 10-point stars, in plane geometry, should follow
 237 the rhythm as indicated in Figure 4A, where w is the width of the rafter. In the rules of traditional Spanish
 238 structural carpentry, it was common for the distance between the boundary rafters of the stars to be equal
 239 to twice the width of these rafters. From there, and inherent to the geometry of the interlacing pattern of
 240 10-point stars, the distance between the side rafters to the stars had to be 3.854 times the thickness,
 241 whereby this measure was obviously obtained through the geometrical layout itself.

242 In order to adapt this pattern to spherical geometry, the carpenter maintained the distance of twice
 243 the thickness in the separation between bordering rafters of stars and modified the canonical separation

244 between stars, with distances between 3.7 to 4.3 times the thickness. As for the upper stack, the 12-point
245 star is generated by the extension of the main rafters of each sector of the dome.

246 It can be presumed that the decision to build the dome was made once the walls of the Ambassadors
247 Hall had been completed, that is, the dome had to be adapted to fit a pre-established dimension. The
248 problem entailed translating such a geometric schema to a spherical shape while taking into account these
249 pre-established dimensions (Figure 4B). To this end, the carpenter had to choose the thickness of the
250 wood to be employed and from there to begin the interlacing pattern. Such a procedure is common in
251 traditional Spanish structural carpentry.



252

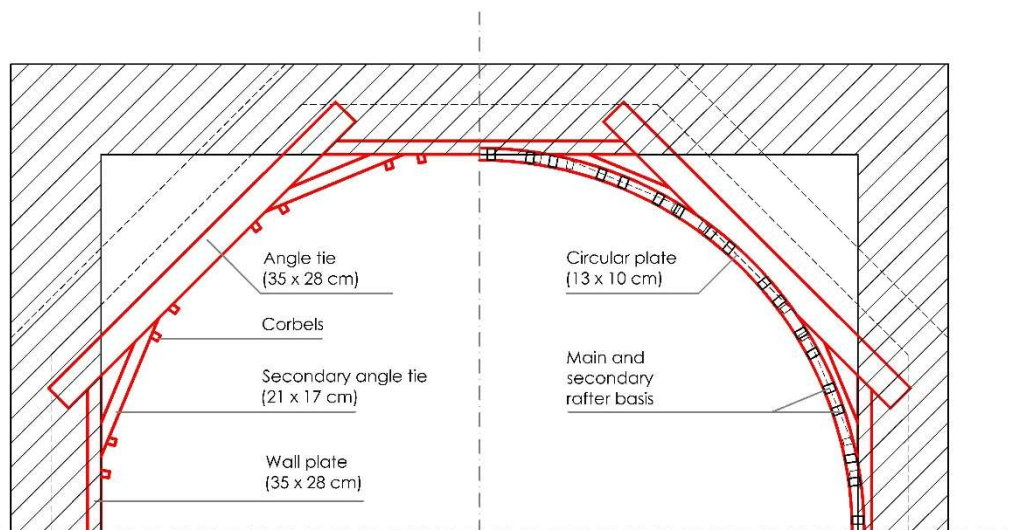
253 *Figure 4: (A) Geometrical pattern of a 10-point interlocking star. (B) Geometric pattern and underlying*
254 *structure in a sector and in upper stack.*

255 Regarding their dimensions, all the pieces that make up the set (both rafters and noggins) have a
256 thickness of approximately 10 cm (the width of the different sections, measured in situ, yield dimensions
257 that range between 9.7 and 10.2 cm). The height of the beams is approximately 14 cm. In addition to the
258 wooden elements, the dome has a wrought-iron tie rod on the exterior arranged along a parallel and
259 located at approximately 15° from the equator of the dome.

260 Finally, it should be borne in mind that currently the keystone of the dome is attached to the
261 covering structure. It remains unknown whether this was its original configuration or the product of an
262 early reform. Elucidating this question will also be the object of structural analysis.

263 **The Supporting Base**

264 The load transfer from the dome to the base walls is performed with 3 orders of elements. In the first
265 place, in the corners, 4 angle ties (35 x 28 cm) are placed at 45° and rest directly on the walls at their
266 respective extremes, thus generating 8 support points. On the walls, there are 4 wall plates (17 x 25 cm).
267 Between these wall plates and the angle ties there are another 8 timbers (secondary angle braces) with a
268 smaller cross-section (21 x 17 cm) connected by metal joints (nails) to both the angle tie and the wall
269 plates. This superposition of elements generates a 16-sided platform on which a circular plate (13 x 10
270 cm) is directly supported upon which the main rafters and secondary rafters of the dome structure rest.



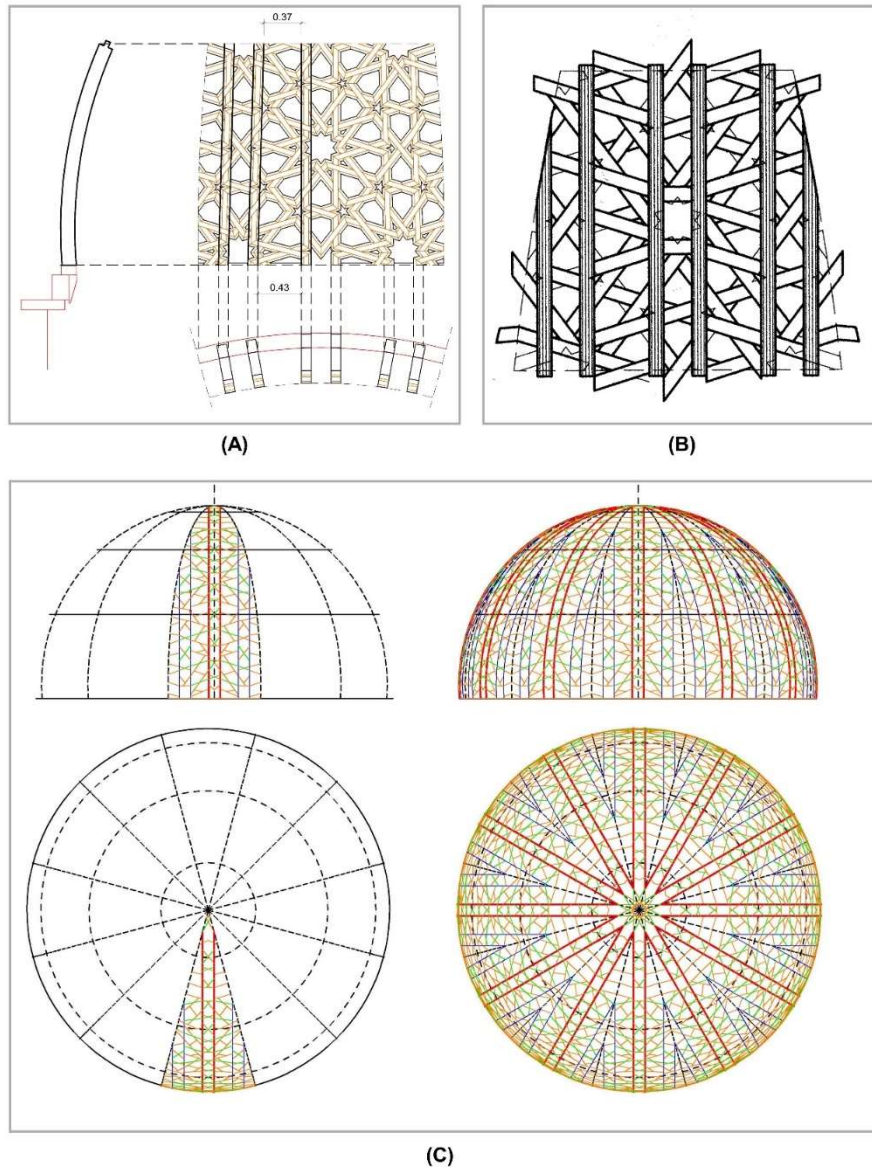
272 *Figure 5: Configuration of the supporting base of the dome.*

273 This circular plate has a projection with respect to the hexadecagonal structure of the base along
274 practically its entire length, and becomes completely in projection, without support, in the area where the
275 wall plate and the angle tie meet. Hence, in order to strengthen the base of the framework, several small
276 corbels have been added (Figure 5).

277 **The Construction of the Stacks of the Dome**

278 The choice of stacks to be prefabricated is based on the geometry of the interlacing pattern. In each
279 stack, it can be appreciated that the lower and upper limits coincide with the mean line of a star, leaving a
280 complete star in the centre of the stack. The definition should have started with the conservation of the
281 canonical layout in the centre of the stack, in the star, and from there the carpenter carried out skilful
282 operations in modifying the distances between adjacent rafters to adapt to the progressive reduction of
283 stack width towards the zenith.

284 Thus, in the lower stack (stack A) (Figure 6A), there are 6 curved rafters that are grouped in pairs
285 and coincide with the location of the stars. Each pair always maintains parallelism and it is the area
286 between these pairs of rafters that absorbs the distortion of the transition from planar to spherical
287 geometry.

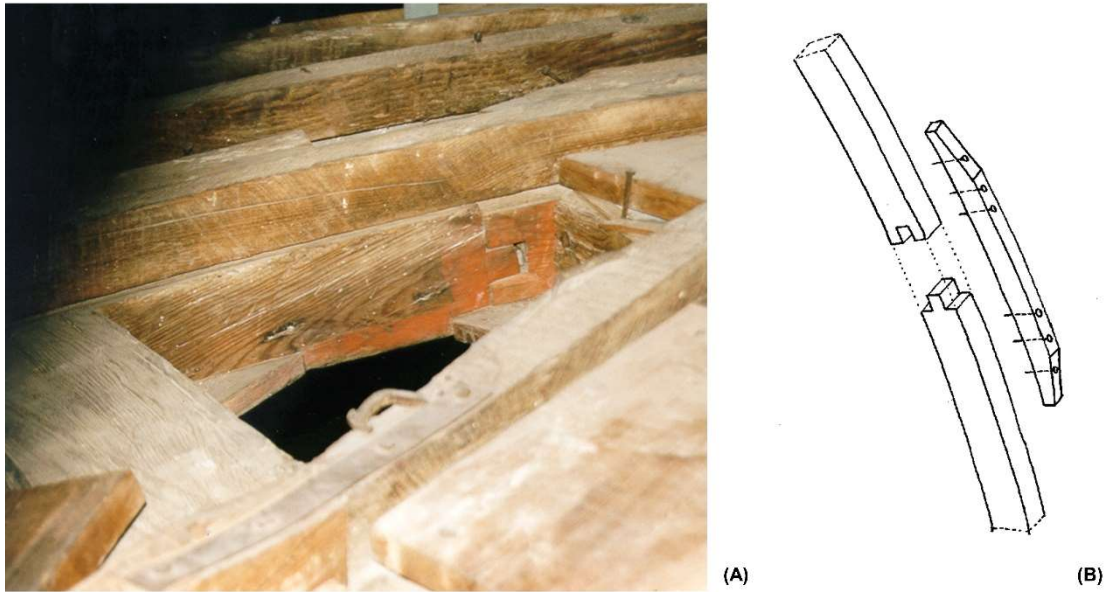


288

289 In the second sector (stack B) (Figure 6B), the location of the main rafters and the entire set of
 290 noggings that unite and stiffen each stack are represented. This analysis of the geometry and underlying
 291 structure has made it possible to create the 3D model which will provide the structural analysis (Figure
 292 6C).

293 **Configuration of the Joints**

294 The joints between the main rafters are of the mortise-tenon type, with the tenon at the head of the
 295 lower element, which fits into a mortise carved into the base of the next rafter (Figure 7a). The joint is
 296 secured with a nailed overlay timber that provides continuity to the joint (Figure 7b).



297

298 *Figure 7: Joints between main rafters in the connection between the stacks.*

299 The union between rafters and noggings is produced through the traditional recessing procedure in
 300 the side wall of the rafter into which the carved tenon of the front of the nogging fits.

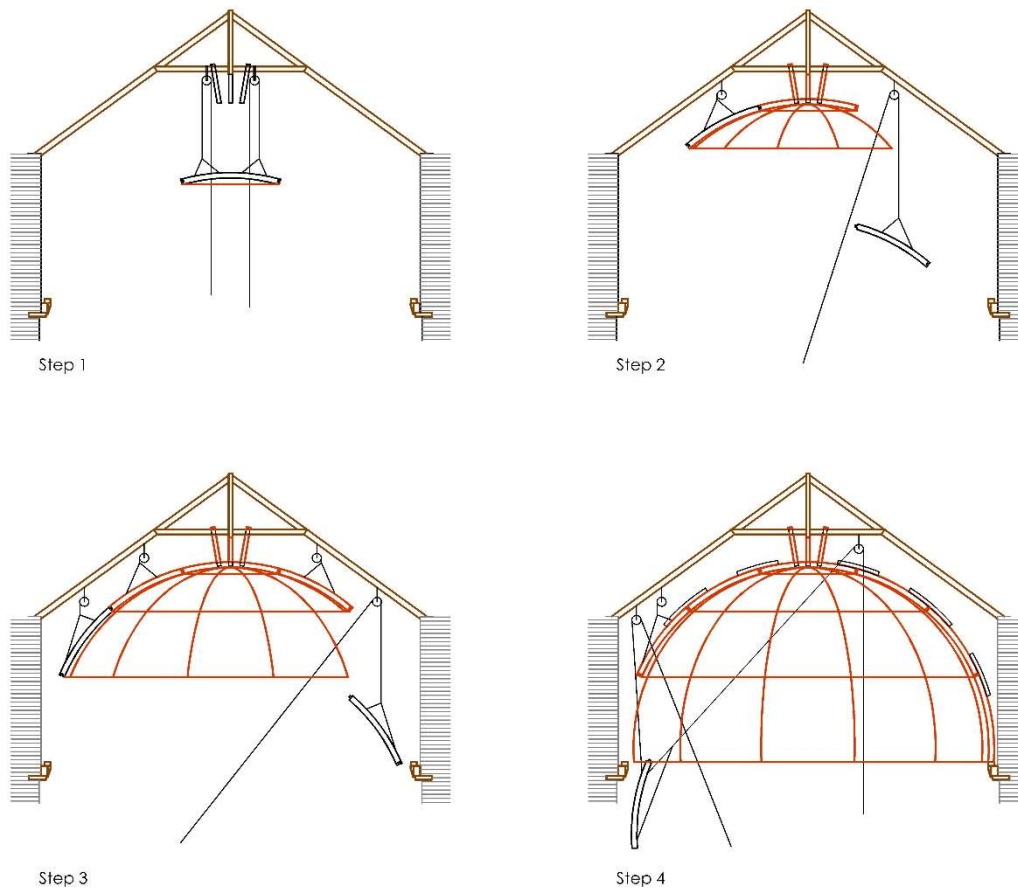
301 The joint at the base of the lower rafters is very straightforward, with only a simple support of the
 302 base of the rafter on the circular plate, without the existence of a recess or similar, except for connection
 303 nails.

304 The profusion of noggings and their multiple directions due to their accommodation to the
 305 interlacing pattern ensures the transverse bracing of the structure on the surface of the dome. The
 306 interlocking existing between the noggings, and between the noggings and the rafters, generates a
 307 structural assembly with sufficient stiffness to maintain its stability even during the procedure of building
 308 the structure.

309 **Hypothesis on the Manufacturing and Assembly Procedure**

310 The analysis of the configuration of the joints between the main rafters indicates that construction
 311 had to be carried out from the upper to the lower level, that is, by placing the circular crowning panel first
 312 and, once this was fixed (to an auxiliary structure), by incorporating the rest of the stacks successively, in
 313 descending order. Indeed, given the configuration of the joints between rafters, in reverse order it would
 314 be impossible to place the key stack by fitting its protruding tenons into the mortise at the top of the
 315 rafters. To this end, a scarf joint would have had to have been made in order to allow such a fit. For the

316 same reason, in this descending assembly, it is only possible to join the lower rafters with the circular
317 plate without any tenons, as is the case here. Thus, the assembly procedure that is represented in Figure 8
318 can be considered.



319
320 *Figure 8: Hypothesis of the construction process of the dome.*

321 **STRUCTURAL BEHAVIOUR**

322 **Models, Hypotheses, and Calculation Procedure**

323 Based on the aforementioned constructive knowledge, the objectives involve the analysis of what
324 makes this dome stable and resistant, since it is a set of elements that, except for the main rafters,
325 principally present pinned joints and with secondary rafters that do not reach the keystone, without
326 presenting any apparent effective subjection with respect to the main rafters.

327 In addition to the current configuration of geometry, links, and loads, two other possibilities are
328 discussed: that the dome could function as an independent structure, without the connection that currently

329 exists with the upper covering; and that the dome could directly support the layers of the roof
330 (waterproofing, covering and wind loads) without the need for said upper structure.

331 In order to meet these objectives, the calculation has been carried out with two geometric models in
332 which various hypotheses of external links, loads to be supported, and internal joint constraints between
333 frames are considered. Model 1 (M1), or simplified geometry, exclusively includes the main rafters and
334 the tie rod. The load corresponding to the spherical triangles is applied on these rafters, an area that would
335 act exclusively as a plementery. This model seeks to ascertain the overall resistant capacity of these main
336 elements and the possibility of admitting full loads of coverage, wind, and snow. Model 2 (M2),
337 fundamental to this study, includes the main rafters and secondary rafters and all the transverse frame-
338 noggings that generate the interlacing pattern.

339 In M1, three hypotheses are proposed (M1a, M1b, M1c), which combine the types of actions and
340 links with the upper roof framing (covering): M1a, actions of their self-weight (dead loads) with the
341 connected (hanging) keystone of the upper structure; M1b, actions with the structure supported only at the
342 base; M1c, actions of their self-weight, permanent cover, wind, and snow loads, with the structure
343 supported only at the base.

344 In M2, four hypotheses are proposed (M2a, M2b, M2c, M2d), which differ regarding whether or not
345 they consider the ability to transmit tensile stresses or moments in the joints between noggings and
346 between these and rafters. In this model, only self-weight loads are taken into account and no connection
347 is considered in the keystone.

348 For the structural analysis of these models, the finite element method (FEM) has been used, which is
349 a widely contrasted procedure for the numerical analysis of this type of structure (Coz Diaz et al., 2012;
350 Chun et al., 2015; Gao and Ohta, 2007; Galassi et al., 2018). The calculation has been developed using
351 SAP2000 software v.22.

352 The geometry is referred to in Figure 10 above, defined from the respective axes of the pieces that
353 pass through the centres of gravity of their sections. Due to the geometric pattern that governs the
354 structure, all the axes are concurrent, and therefore no incorporation of additional frames is necessary to
355 model eccentricities.

356 **Material Properties and Actions Considered**

357 Identification tests carried out on the wood of the structure during restoration work at the beginning
358 of the 21st century indicate that the oldest elements are European larch (*Larix decidua Mill.*), whereby
359 Scots pine (*Pinus sylvestris L.*) was used in the renovation repair work of the mid-19th century (Fernández
360 Aguilera and Pérez Ferrer, 2000).

361 In order to obtain the resistant properties of larch, the UNE EN-1912 (AEN/CTN-56, 2012) has been
362 used. According to this standard, larch wood can be assigned to resistant classes ranging from C14 to C30
363 depending on its origin and its singularities. In the case of this dome, since it is an element of special
364 importance, it is appreciated that the wood was specifically selected. Proof of this appears in the reduced
365 diameter of all types of knots (simple knots, splay knots, and overlapping knots) in relation to the
366 dimensions of the pieces. Therefore, using the visual grading rules of the various European countries
367 where larch wood could come from, it can be considered that it would always be classifiable to at least an
368 intermediate grade (ST2 of French origin, S2 from Italy, or T2 from the Netherlands), and could be
369 assigned to at least resistant class C22 or C24. In this study, the wood has been conservatively considered
370 as class C22. For the characteristic strength and stiffness properties, the values indicated in UNE EN-338
371 (AEN/CTN-56, 2017) are used. The permanent and imposed loads, as well as the load combinations and
372 load factors have been determined based on Eurocode 1 (Technical Committee CTN 140, 2019).

373 **Structural Analysis: Hypotheses, Connections, and Stresses.**

374 *Simplified model analysis (M1)*

375 First of all, the resistant capacity of the dome is studied, made up exclusively of the twelve pairs of
376 main rafters that have continuity from the base to the keystone. This continuity is guaranteed by the type
377 of connection between stacks as explained in the previous section (Figure 11). In the model, although the
378 noggings are not included, their effect is considered by coercing the lateral instability of the rafters.
379 Furthermore, movement is restricted to the area where the metal tie rod is located. The results obtained
380 for the 3 hypotheses are (Table 1):

381

382

383

384 *Table 1. Results obtained for the hypotheses considered*

	M1a:	M1b:	M1c:
	Self-weight only. Structure is connected in the crown.	Self-weight only. Structure is free in the crown.	Self-weight, covering, wind, and snow. Structure is free in the crown.
Nmax	-9.7 kN (upper stack)	-12.6 kN (upper stack)	-25.9 kN (upper stack)
Mmax	-1.02 mkN (upper stack)	0.77 mkN (upper stack)	-14.65 mkN (upper stack)
Vmax	2.25 kN (tie rod)	1.73 kN (tie rod)	4.45 kN (supporting base)
Safety factor	0.13	0.10	1.84

385

386 The result shows that the structure is stable. However, the safety factor shows that the design
 387 strength is exceeded if it supports the full load of the covering. In contrast, the structure presents
 388 sufficient safety factor in the case of supporting only its self-weight and the weight of the upper covering.
 389 The values of the maximum stresses obtained are of a similar magnitude in Hypotheses M1a and M1b,
 390 and are therefore independent of whether the dome is hanging from an upper structure or not. This
 391 analysis thereby reveals that the connection in the crown is not necessary for its stability and resistance,
 392 and therefore this connection may have been absent in its original configuration.

393 *Analysis of the complete structural model (M2)*

394 In this model, all the elements of the dome are considered: the main rafters, the secondary rafters,
 395 and the noggings distributed on the spherical surface.

396 A singularity of this structure is that the secondary rafters converge with each other and are only
 397 supported at their base. With this configuration, they would be unable to absorb any load, which
 398 otherwise would constitute a mechanism, and hence the stability provided by the noggings to the
 399 structural assembly is to be analysed.

400 The joints between noggings and rafters are produced with a mortise into which the tenon is
 401 inserted. Observation in situ has revealed no existence of nails or similar that would guarantee a possible
 402 transmission of tension stress. Thus, these connections can have compression transmission capacity,

403 practically zero tension transmission, and a certain capacity to prevent rotation. For the analysis, four
 404 hypotheses have been made that consider different internal constraints (fixed or pinned) and consider the
 405 ability or not to admit tension stress.

406 Table 2 describes the hypotheses and the result, whether it be consistent or not, of the structural
 407 behaviour of each model. The external restraints have been considered as free-bearing supports and the
 408 structure without connection in the keystone, supporting only its self-weight.

409 *Table 2. Hypothesis for joint connections and frame stresses in Model 2*

Structural hypothesis	Connections (Joint constraints)	Frame stress	Results of the analysis	Comments
M2a	Fixed	No Tension (compression)	Consistent	The result is consistent: the structure is stable.
M2b	Fixed	Tension + Compression	Consistent	The result is consistent: maximum vertical deformation occurs in the upper stack.
M2c	Pinned	No Tension (compression)	Non-consistent	The structure is unstable: its deformation is not as a rigid body.
M2d	Pinned	Tension + Compression	Non-consistent	As in the previous case, the deformation of the structure is not consistent.

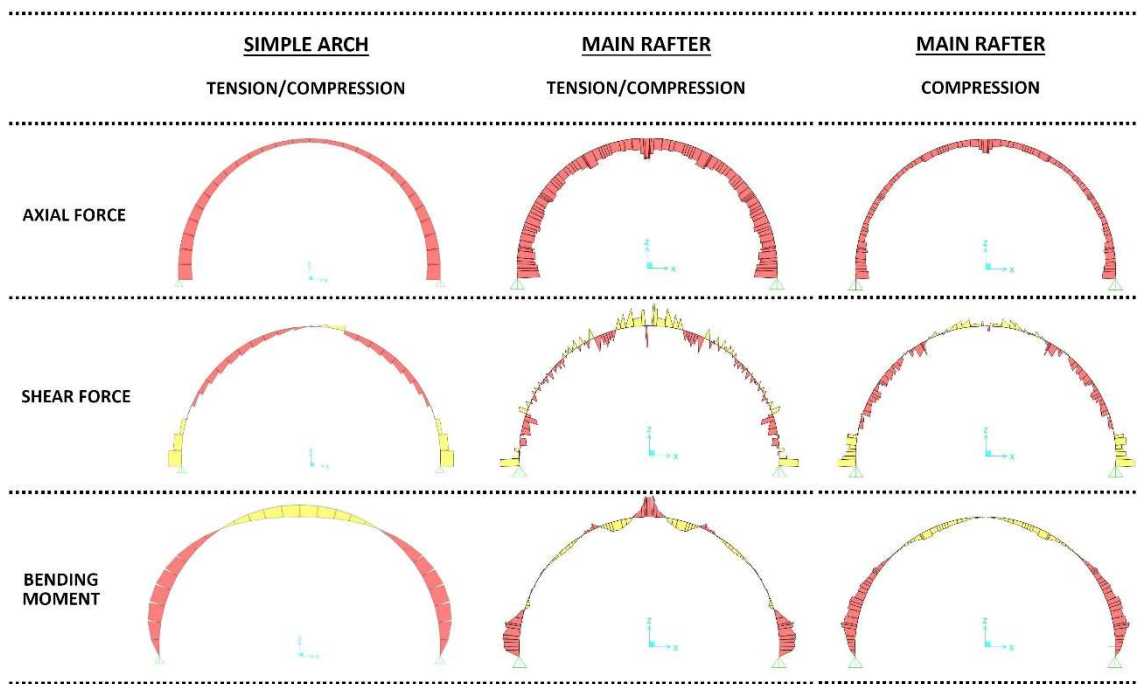
410

411 From Table 2 it can be deduced that the dome is only stable if the connections between rafters and
 412 noggings, as well as between the noggings themselves, are considered rigid. If the inability of the
 413 noggings to transmit tension stress is added to this, then the only viable hypothesis is Hypothesis M2a. It
 414 is therefore essential to ensure that the analytical model reproduces physical reality, to determine whether
 415 the moments that occur in the joints can be resisted by said joints. The structural analysis indicates that
 416 the maximum design shear in the joints between rafters and noggings is produced in the confluence zone
 417 between the longest secondary rafters ($V_d = 0.43$ kN; $M_d = 0.015$ mkN). The maximum bending moment
 418 is generated in the noggings located in the contact between the main rafters and the upper sector ($V_d =$
 419 0.17 kN; $M_d = 0.045$ mkN).

420 Recent publications delve into the analysis of the resistance capacity in mortise-tenon-type joints (Li
 421 et al., 2015; Yang, Yu, and Law, 2020; Kunecký et al., 2016; Chen, Qiu, and Lu, 2016). Considering
 422 exclusively the tenon cross-section (30 x 100 mm) therefore, without considering increases in strength
 423 derived from friction and joint operation due to compression of the joint base, a load capacity of 0.21
 424 mkN is obtained for the bending moment and of 9.4 kN for the shear force. This indicates that the tenon
 425 itself has the capacity to absorb moments of at least 4.7 times the acting worst bending moment and 5.4
 426 times the maximum shear force.

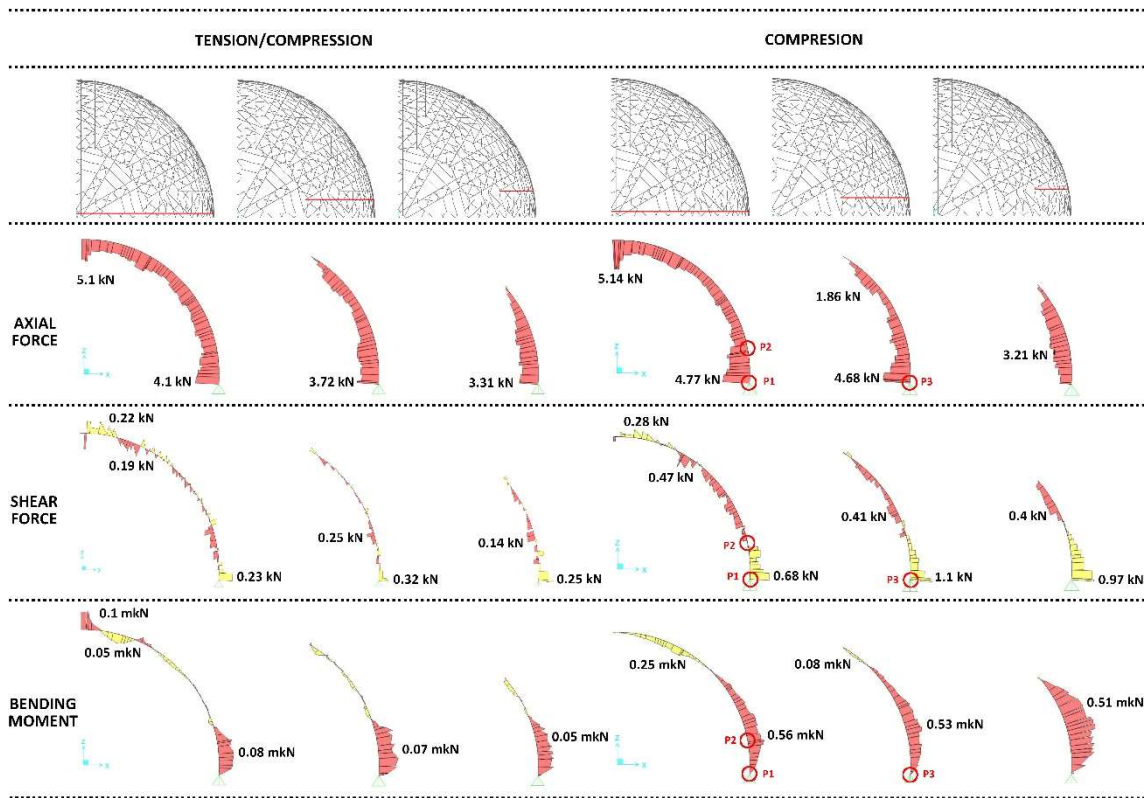
427 Based on the results indicated, it can be stated that the existing joints can behave as effective fixings,
 428 as indicated in Eurocode 5 (Technical Committee CTN 140 2016, Art. 5.4.2.). This circumstance
 429 demonstrates the fundamental contribution of the noggings to the stability and resistance of the whole.

430 In order to validate the adopted calculation model, for the cases that present coherent behaviour
 431 (Table 2, M2a and M2b), the distribution of forces in one of the main rafters has been compared with that
 432 of a theoretical simple arch of the same dimension (Figure 9). It is evident that, with the rafters working
 433 only in compression, the behaviour of the rafters in our model is similar to that of the simple arch, as was
 434 the case in the simplified model M1b. This result is consistent with the type of carpentry joints in the
 435 dome nodes.



436
 437 *Figure 9: Results obtained in the analysis of the main isolated rafter.*

438 Although the axial forces are similar in the two cases, the model with frames only in compression
 439 (M2a) presents higher values for both the shear forces and the bending moments. Figure 10 shows the
 440 forces that occur in the main rafters and in the two secondary rafters, in the M2a and M2b models.



441
 442 *Figure 10. Results obtained in the analysis of M2a (right) and M2b (left) models. Circles highlight points*
 443 *where the safety factor is obtained.*

444 Table 3 indicates the safety factors for the frames with maximum forces in the hypothesis of
 445 frames only in compression (M2a), using the Ultimate Limit States procedure of Eurocode 5. The results
 446 reflect that the resistance of the sections utilised is far from exhausted, with only 19% of its resistant
 447 capacity being employed in the worst case scenario (combination of axial and bending moment in point
 448 2).

449

450

451

452

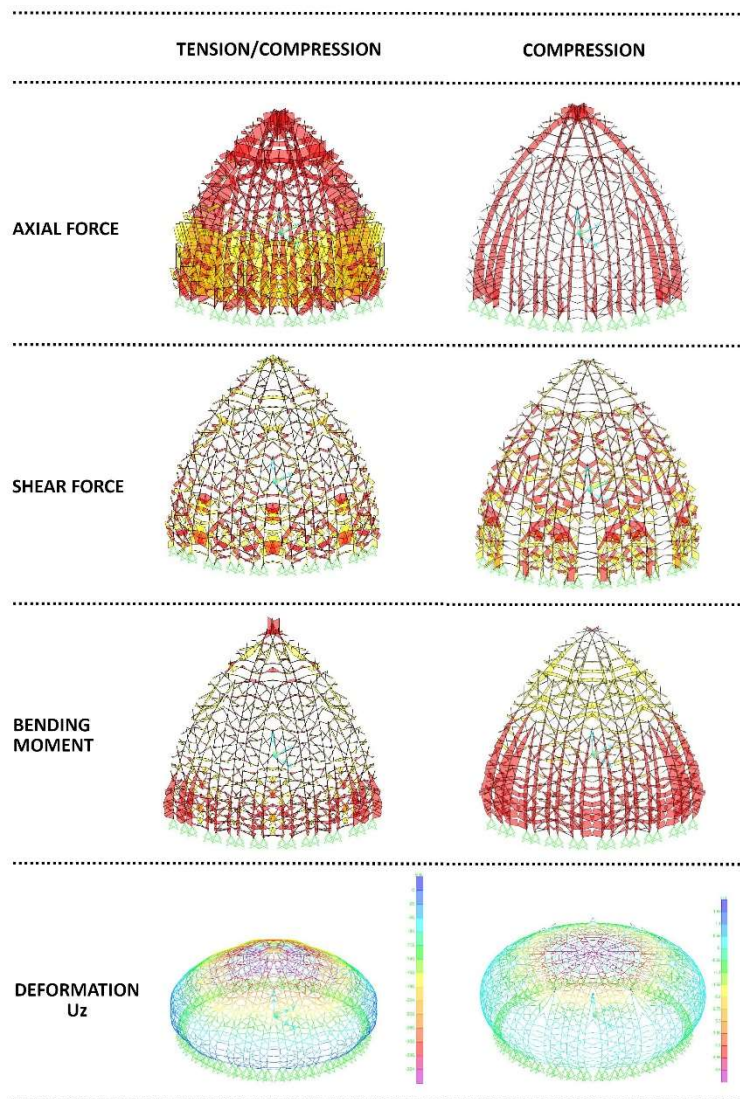
453

454 Table 3. Safety factor analysis on main rafters

								Safety Factor			
Forces/Bending Moment					Stresses (kN/m ²)			N _d , M _d	V _d	N _d , M _d	V _d
Point	K _{mod}	N _d (kN)	V _d (kN)	M _d (mkN)	σ _{c,0,d}	σ _{m,y,d}	τ _{max}	C14		C22	
1	0.6	-4.77	0.68	0	-340.71	0	108.74	0.0021	0.08	0.0005	0.04
2	0.6	-3.11	0	0.56	-222.14	1714.29	0.00	0.1866	0.00	0.0701	0.00
3	0.6	-4.68	1.1	0	-334.29	0	175.91	0.0020	0.13	0.0005	0.06

455

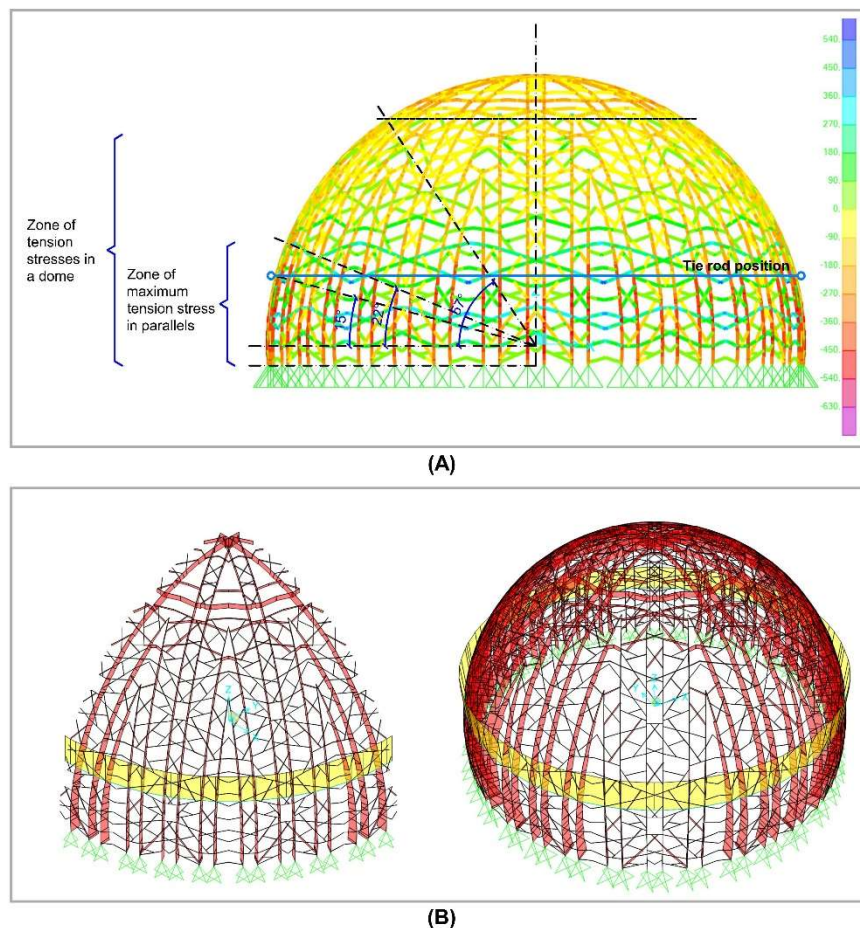
456 The three-dimensional analysis of the forces (Figure 11) shows how, with frames only under compression
 457 (M2a), all the rafters work as a succession of arches, collaborating together to drive the gravitational
 458 loads to the base of the structure.



459

460 Figure 11: 3D internal forces diagram on a dome sector for M2a (right) and M2b (left) models

461 Likewise, Hypothesis M2a shows that the maximum transverse tension stresses are generated
462 between the 22° parallel and the spring line of the structure (Figure 12A). In the dome of the Hall of
463 Ambassadors there is a tie rod placed at the height of the 15° parallel, in the area where the greatest
464 horizontal deformation occurs (Figure 11). This position of the tie rod coincides with point P2 (Figure 10)
465 in which the maximum bending moment occurs in the rafters. The mitre joint between the noggings
466 makes it impossible to transmit tension stresses in the direction of the parallels since there are no metal
467 connectors. The tie rod absorbs these tension stresses and maintains the stability of the dome by
468 preventing the separation between the different sectors. In every sector, the interlacing of the noggings
469 increases the stiffness in their surface, which allows a unitary behaviour as solid-rigid, thereby enabling
470 the assembly process by sectors as explained in Figure 8.



471
472 *Figure 12: (A) Stresses on the dome for the M2a model and location of the tie rod. (B) Axial forces on*
473 *Model M2a considering the presence of the tie rod.*

474 In an analysis of the upper stack, the noggings that delimit it should function as a compression ring
475 to ensure the overall stability of the structure. This occurs in the hypothesis with frames only under

476 compression (M2a) when the tie rod is incorporated. The result (Figure 12B) presents total coherence: the
477 frames of the upper spherical stack work under compression, thereby granting the rafters the
478 responsibility of transmitting the gravitational load, with the tie rod resisting the tension stresses
479 generated in the dome. The compressive force in the frames that limit the upper stack, of 1.65 kN, is
480 much lower than their resistance to axial capacity, of 92.3 kN.

481 The maximum reactions in the rafters in the base of the structure are $R_{x,d} = 0.30$ kN; $R_{y,d} = 0.30$ kN;
482 $R_{z,d} = 4.0$ kN, with the global vertical reaction at the base being 253.1 kN. The maximum axial force in
483 the tie is $N_d = 9.1$ kN. Given the age of the tie rod, assuming a resistance for a steel with practically no
484 carbon content of 180 N/mm², a circular section $\phi 8$ or a square section of 8×8 mm² is sufficient to
485 withstand the axial force. Given that the dome was built in 1427, the original solution to resist these
486 tension stresses could have consisted of a series of staggered frames arranged transversely to the main
487 rafters. In this hypothesis, the current metal tie rod would have been incorporated in a subsequent
488 intervention.

489 *Analysis of the model without a covering*

490 Having verified that the only congruent hypotheses are those of M2a and M2b, and that Hypothesis
491 M2a reliably represents its structural behaviour, an analysis is carried out of the possibility that the
492 structure can work autonomously, that is, without an additional upper framework, thereby supporting the
493 dead load of the covering, as well as those of snow and wind. The results indicate that, as long as the
494 joints only transmit compressions as in Hypothesis M2a, then the dome behaves as a mechanism against
495 horizontal actions. Therefore, it is concluded that from its origin there had to be some type of upper
496 covering similar to the one that exists today.

497 **CONCLUSIONS**

498 The wooden dome of the Hall of Ambassadors of the Alcázar of Seville, dating from 1427, is one of
499 the rare examples of wooden domes built following the guidelines of the Spanish medieval carpentry
500 tradition. This, in addition, is the oldest specimen of those that are still preserved. The analysis of the
501 historical evolution of the construction of wooden domes reveals that there is no structure with similar
502 characteristics in other countries.

503 The geometric and constructive analysis has made it possible to ascertain both the configuration of
504 the joints and the construction process that could be followed for the construction of this dome. It is
505 evident that it was performed by means of independent prefabricated sectors, whereby a unique assembly
506 process was followed for its construction. This began by lifting and assembling the upper spherical stack
507 to which the lower stacks were successively assembled until the spring line of the structure was reached.

508 The models and calculation hypotheses adopted, which have been analysed using FEM, enable
509 the structural behaviour of the dome to be determined. It has been verified that the stability of the set can
510 be explained, on the one hand, due to the constructive continuity of the 12 main rafters, and, on the other
511 hand, through the fundamental structural function exercised by the noggings. These elements follow the
512 layout of the lacework generated by the interlacing pattern geometry present in the cupola and unite the
513 main rafters in multiple directions. The interlacing between the numerous noggings provides stability to
514 the set, revealing not only the decorative but also the resistant role of these pieces, which generate a
515 bracing of the structure on the surface of each panel. This function of the noggings would be especially
516 relevant in absorbing the forces generated during the lifting and assembly process of the different stacks
517 during the construction of the framework.

518 The structural analysis has revealed the impossibility of transmission of tension stresses due to the
519 mortise-tenon joints existing between noggings and rafters. Likewise, it is shown that these joints have a
520 load capacity greater than 1.5 times that corresponding to the combination of the applied force and
521 moment, and hence it can be considered that they behave as fixed joints in the face of acting actions. The
522 frames most requested in the structure are the main rafters, the longest (those that reach the zenith of the
523 dome) being those that support the greatest forces. Despite this, the safety factor obtained indicates that
524 they work at 19% of their capacity. Therefore, with all the frames in a good state of preservation, the dead
525 load, which currently corresponds exclusively to the sheathing, could be increased to 5 kN/m².

526 The structural behaviour of the spherical framework implies the appearance of maximum tension
527 stresses from the 22° parallel. Inability to absorb the tension stress of the noggings would imply the
528 collapse of the structure, which is why the fundamental role of the metal tie rod (tension ring), capable of
529 absorbing these tension stresses, is demonstrated. This tie rod is placed at the 15° parallel and coincides
530 with the area of greatest transverse deformation of the structure.

531 To conclude, delving into the constructive and structural study of historical architecture has the
532 value of revealing not only the construction techniques and procedures, but also the knowledge treasured
533 in each age by master builders. Furthermore, a full understanding of the functionality of its different
534 components provides useful information towards perfecting and improving the conservation and
535 maintenance processes necessary to ensure their state of preservation. Likewise, from the point of view of
536 current structural design, given this knowledge, it is possible to design optimal structural typologies based
537 on the adaptation of its construction system, thereby improving those features that are in need of
538 adjustment.

539 **DATA AVAILABILITY STATEMENT**

540 Some or all data, models, or code that support the findings of this study are available from the
541 corresponding author upon reasonable request.

542 **REFERENCES**

- 543 AEN/CTN-56. (2012). “UNE-EN 1912:2012. Structural Timber. Strength Classes. Assignment of Visual
544 Grades and Species.” Madrid: AENOR.
- 545 AEN/CTN-56. (2017). “UNE-EN 338:2016. Structural Timber. Strength Classes.” Madrid: AENOR.
- 546 al-Ratrout, Haitem. 2017. “Sacred Architecture of the Rock : An Innovative Design Concept and
547 Iconography in Al-Aqsa Mosque.” Milel ve Nihal 14 (2): 49–73.
548 <https://doi.org/10.17131/milel.377618>.
- 549 Almagro, Antonio. (2001). “Un Aspecto Constructivo de Las Bóvedas En Al-Andalus.” Al-Qantara XXII
550 (1).
- 551 Álvarez, Rodrigo. (1699). Breve Compendio de La Carpintería y Tratado de Lo Blanco Con Algunas
552 Cosas Tocante a La Iometría y Puntas Del Compas.
- 553 Ashkan, Maryam, and Yahaya Ahmad. (2010). “Discontinuous Double-Shell Domes through Islamic Eras
554 in the Middle East and Central Asia: History, Morphology, Typologies, Geometry, and
555 Construction.” Nexus Network Journal 12 (2): 287–319. <https://doi.org/10.1007/s00004-010-0013-9>.

- 556 Bails, Benito. (1796). *Elementos de Matemática*. Por D. Benito Bails. Tom. IX. Parte I. Que Trata de La
557 Arquitectura Civil. Segunda Edición Corregida Por El Autor. 1st ed. Madrid: Imprenta de la viuda
558 de D. Joaquin Ibarra.
- 559 Chen, Chunchao, Hongxing Qiu, and Yong Lu. (2016). “Flexural Behaviour of Timber Dovetail Mortise-
560 Tenon Joints.” *Construction and Building Materials* 112: 366–77.
561 <https://doi.org/10.1016/j.conbuildmat.2016.02.074>.
- 562 Chun, Qing, Koenraad Van Balen, Jianwu Pan, and Lanxiang Sun. (2015). “Structural Performance and
563 Repair Methodology of the Wenxing Lounge Bridge in China.” *International Journal of*
564 *Architectural Heritage* 9 (6): 730–43. <https://doi.org/10.1080/15583058.2015.1041191>.
- 565 Coz Diaz, Juan José Del, Paulino José García Nieto, Felipe Pedro Álvarez Rabanal, and Alfonso
566 Gerónimo Lozano Martínez-Luengas. (2012). “Optimization Based on Design of Experiments
567 (DOE) Using Finite Element Model (FEM) Analysis Applied to Retrofitting the Church of
568 Baldornon, Spain.” *International Journal of Architectural Heritage* 6 (4): 436–51.
569 <https://doi.org/10.1080/15583058.2011.580825>.
- 570 Fernández Aguilera, Sebastián, and Juan Carlos Pérez Ferrer. (2000). “Restauración de La Cúpula Del
571 Salón de Embajadores.” *Apuntes Del Alcázar de Sevilla* 1 (may): 74–85.
- 572 Fregonese, Luigi, Laura Taffurelli. (2009). “3D Model for the Documentation of Cultural Heritage : The
573 Wooden Domes of St . Mark ’ S Basilica in Venice.” *International Archives of the Photogrammetry,*
574 *Remote Sensing and Spatial Information Sciences - ISPRS Archives* 38 (5).
- 575 Galassi, Stefano, Nicola Ruggieri, Letizia Dipasquale, and Giacomo Tempesta. (2018). “Assessment of
576 the Moroccan Vernacular Timber Roof: A Proposal for an Eco-Friendly Strengthening System.”
577 *Journal of Architectural Conservation* 24 (3): 224–48.
578 <https://doi.org/10.1080/13556207.2018.1545105>.
- 579 Gao, Ying, and Masamitsu Ohta. (2007). “Deformation Analysis of Timber-Framed Panel Dome
580 Structure I: Simulation of a Dome Model Connected by Elastic Springs.” *Journal of Wood Science*
581 53 (2): 100–107. <https://doi.org/10.1007/s10086-006-0823-2>.

- 582 García Berruguilla, Juan. (1747). Verdadera Práctica de Las Resoluciones de La Geometría Sobre Sobre
583 Las Tres Dimensiones Para Un Perfecto Arquitecto. 1st ed. Madrid: Imprenta de Lorenzo Francisco
584 Mojados.
- 585 González de León, Félix. (1844). Noticia Artística de Todos Los Edificios de Esta Muy Noble Ciudad de
586 Sevilla. Facsimile. Sevilla: Extramuros, 1973. [http://www.cervantesvirtual.com/obra/noticia-](http://www.cervantesvirtual.com/obra/noticia-artistica-historica-y-curiosa-de-todos-los-edificios-publicos-sagrados-y-profanos-de-esta-muy-noble-muy-leal-muy-heroica-e-invicta-ciudad-de-sevilla-y-de-muchas-casas-particulares/)
587 [artistica-historica-y-curiosa-de-todos-los-edificios-publicos-sagrados-y-profanos-de-esta-muy-](http://www.cervantesvirtual.com/obra/noticia-artistica-historica-y-curiosa-de-todos-los-edificios-publicos-sagrados-y-profanos-de-esta-muy-noble-muy-leal-muy-heroica-e-invicta-ciudad-de-sevilla-y-de-muchas-casas-particulares/)
588 [noble-muy-leal-muy-heroica-e-invicta-ciudad-de-sevilla-y-de-muchas-casas-particulares/](http://www.cervantesvirtual.com/obra/noticia-artistica-historica-y-curiosa-de-todos-los-edificios-publicos-sagrados-y-profanos-de-esta-muy-noble-muy-leal-muy-heroica-e-invicta-ciudad-de-sevilla-y-de-muchas-casas-particulares/).
- 589 Jousse, Mathourin. (1627). Le Theatre de L'Art de Charpenterie. 1st ed. Paris: F. Jollain.
- 590 Kunecký, Jiří, Anna Arciszewska-Kędzior, Václav Sebera, and Hana Hasníková. (2016). "Mechanical
591 Performance of Dovetail Joint Related to the Global Stiffness of Timber Roof Structures." *Materials*
592 *and Structures/Materiaux et Constructions* 49 (6): 2315–27. [https://doi.org/10.1617/s11527-015-](https://doi.org/10.1617/s11527-015-0651-1)
593 [0651-1](https://doi.org/10.1617/s11527-015-0651-1).
- 594 Li, Xiaowei, Junhai Zhao, Guowei Ma, and Shuanghua Huang. (2015). "Experimental Study on the
595 Traditional Timber Mortise-Tenon Joints." *Advances in Structural Engineering* 18 (12): 2089–2102.
596 <https://doi.org/10.1260/1369-4332.18.12.2089>.
- 597 López de Arenas, Diego. (1619). Primera y Segunda Parte de Las Reglas de La Carpintería. 1st ed.
598 Sevilla: Luis Estupiñán.
- 599 López de Arenas, Diego. (1633). Breve Compendio de La Carpintería de Lo Blanco y Tratado de
600 Alarifes. 1st ed. Sevilla: Luis Estupiñán.
- 601 Misztal, Barbara. (2018). *Wooden Domes: History and Modern Times*. 1st ed. Cham: Springer.
- 602 Muet, Pierre Le. (1681). *Manière de Bien Bastir Pour Toutes Sortes de Personnes*. 2nd ed. Cologne:
603 François Jollain.
- 604 Necipoğlu, Gülru. (2008). "The Dome Of The Rock As Palimpsest: 'Abd Al-Malik's Grand Narrative
605 And Sultan Süleyman's Glosses." In *Muqarnas, Volume 25 Frontiers of Islamic Art and*
606 *Architecture: Essays in Celebration of Oleg Grabar's Eightieth Birthday*, 1st ed., 17–106. Leiden
607 (The Netherlands): Brill. <https://doi.org/10.1163/ej.9789004173279.i-396.13>.
- 608 Nuere Matauco, Enrique. (1990). *La Carpintería de Lazo: Lectura Dibujada Del Manuscrito de Fray*
609 *Andrés de San Miguel*. 1st ed. Málaga: Colegio Oficial de Arquitectos de Andalucía Oriental.

610 Nuere Matauco, Enrique, Ángel Candelas-Gutierrez, and Javier De Mingo García. (2020). “Análisis
611 Constructivo de La Cúpula de Madera Del Desaparecido Palacio de Los Cárdenas En Torrijos (S.
612 XV).” *Informes de La Construcción* 72 (559): 353. <https://doi.org/10.3989/ic.71019>.

613 Piana, Mario. (2009). “San Giorgio Maggiore e Le Cupole Lignee Lagunari.” *Annali Di Architettura* 21:
614 79–90.

615 San Miguel, Fray Andrés de. n.d. *Untitled Manuscript*. Conserved in the library of the University of
616 Austin (Texas). Facsimile reproduction in Nuere Matauco, Enrique. (1990). *La Carpintería de Lazo:
617 Lectura Dibujada Del Manuscrito de Fray Andrés de San Miguel*. 1st ed. Málaga: Colegio Oficial de
618 Arquitectos de A.

619 Tavakoli Dinani, Ali, Solmaz Sadeghi, and Paulo B. Lourenço. (2019). “A Double Dome through the
620 Ages. Building Technology and Performance of Estahan Shah Mosque’s Dome.” In *Structural
621 Analysis of Historical Constructions*, edited by R. Aguilar, 1st ed., 18:1949–58.
622 <https://doi.org/10.1007/978-3-319-99441-3>.

623 Technical Committee CTN 140. (2016). “Eurocode 5: Design of Timber Structures. Part 1-1: General -
624 Common Rules and Rules for Buildings (UNE-EN 1995-1-1).” Madrid: AENOR.

625 Technical Committee CTN 140. (2019). “Eurocode 1: Actions on Structures - Part 1-1: General Actions -
626 Densities, Self-Weight, Imposed Loads for Buildings. Amendment 1: National Annex (UNE-EN
627 1991-1-1).” Madrid: AENOR.

628 Varela de Salamanca, Juan. (1527). *Ordenanzas de Sevilla : Recopilación de Las Ordenanzas de La Muy
629 Noble y Muy Leal Ciudad de Sevilla, de Todas Las Leyes y Ordenamientos Antiguos y Modernos*.
630 1st ed. Sevilla: Juan Varela de Salamanca.

631 Yang, Qingshan, Pan Yu, and Siu seong Law. (2020). “Load Resisting Mechanism of the Mortise-Tenon
632 Connection with Gaps under in-Plane Forces and Moments.” *Engineering Structures* 219
633 (September): 110755. <https://doi.org/10.1016/j.engstruct.2020.110755>.

634
